Genome-wide association study meta-analysis of neurofilament light (NfL) levels in blood reveals novel loci related to neurodegeneration

Check for updates

Shahzad Ahmad [1,2,29], Mohammad Aslam Imtiaz [3,29], Aniket Mishra [4], Ruiqi Wang[5], Marisol Herrera-Rivero [6,7], Joshua C. Bis [8], Myriam Fornage [9], Gennady Roshchupkin [1], Edith Hofer[10,11], Mark Logue [12,13], W. T. Longstreth Jr[14], Rui Xia[9], Vincent Bouteloup[4], Thomas Mosley[15], Lenore J. Launer [16], Michael Khalil [17], Jens Kuhle[18], Robert A. Rissman[19], Genevieve Chene[4], Carole Dufouil [4], Luc Djoussé[20], Michael J. Lyons[21], Kenneth J. Mukamal [22], William S. Kremen [23], Carol E. Franz [23], Reinhold Schmidt[10], Stephanie Debette [4,24], Monique M. B. Breteler [3,25], Klaus Berger[26], Qiong Yang [5], Sudha Seshadri [5,27], N. Ahmad Aziz [3,28,30], Mohsen Ghanbari [1,30] & M. Arfan Ikram [1,30] ✉

Neurofilament light chain (NfL) levels in circulation have been established as a sensitive biomarker of neuro-axonal damage across a range of neurodegenerative disorders. Elucidation of the genetic architecture of blood NfL levels could provide new insights into molecular mechanisms underlying neurodegenerative disorders. In this meta-analysis of genome-wide association studies (GWAS) of blood NfL levels from eleven cohorts of European ancestry, we identify two genome-wide significant loci at 16p12 (*UMOD)* and 17q24 (*SLC39A11*). We observe association of three loci at 1q43 (*FMN2*), 12q14, and 12q21 with blood NfL levels in the meta-analysis of African-American ancestry. In the trans-ethnic meta-analysis, we identify three additional genome-wide significant loci at 1p32 (*FGGY*), 6q14 (*TBX18*), and 4q21. In the post-GWAS analyses, we observe the association of higher NfL polygenic risk score with increased plasma levels of total-tau, Aβ-40, Aβ-42, and higher incidence of Alzheimer's disease in the Rotterdam Study. Furthermore, Mendelian randomization analysis results suggest that a lower kidney function could cause higher blood NfL levels. This study uncovers multiple genetic loci of blood NfL levels, highlighting the genes related to molecular mechanism of neurodegeneration.

Blood levels of the neurofilament light chain (NfL) have emerged as a robust biomarker of neuro-axonal injury and are increased in a range of neuro-degenerative disorders including Alzheimer's disease (AD), Parkinson's disease (PD), Huntington's disease, amyotrophic lateral sclerosis (ALS), and multiple sclerosis[1]. NfL proteins are expressed in the cytoplasm of neurons where they confer structural stability to the cytoskeleton of neurons[1,2]. Under normal physiological conditions, NfL proteins are continuously released from the axoplasm into circulation in an age-dependent manner[3], whereas neuro-axonal damage has been associated with increased release of NfL in the neuronal extracellular space[3,4]. NfL proteins may diffuse into the

cerebrospinal fluid (CSF) and circulation[5]. Central nervous system origin of the blood NfL levels is also supported by earlier studies demonstrating a strong correlation between CSF and blood NfL levels[3,6]. The advent of highly sensitive assays enables quantification of blood NfL levels[5], thereby facilitating its clinical implementation as a biomarker of neuro-axonal injury and neurodegeneration[7,8]. Identifying the genetic basis of the NfL in blood could therefore provide a better understanding of the biological pathways underlying axonal damage and facilitate identification of shared molecular mechanisms contributing to neuronal loss across neurodegenerative disorders.

A full list of affiliations appears at the end of the paper. ✉e-mail: m.a.ikram@erasmusmc.nl

1

Previously, three modest size genome-wide association studies (GWAS) were performed to identify the genetic variants associated with plasma and CSF levels of NfL in the Alzheimer's Disease Neuroimaging Initiative (ADNI) cohort[9–11]. Hong et al. reported the genome-wide significant association of variant rs1548884 within the *TMEM106B* gene with CSF levels of NfL[11]. Moreover, genetic variants near the *ADAMTS1* gene have been identified as being associated with CSF NfL levels[9], and blood based studies have shown sub-threshold associations of the *LUXP2* and *GABRB2* genes with plasma NfL levels[10]. To uncover the underlying genetic factors of blood NfL levels, studies with substantially larger sample sizes across different ancestries are warranted.

In the current study, we therefore performed a GWAS meta-analysis based on the findings from 11 cohorts of the Cohorts for Heart and Aging Research in Genomic Epidemiology (CHARGE) consortium including people from both European and African-American ancestry. Furthermore, we performed a range of post-GWAS investigations, including expression quantitative trait loci (eQTLs) lookups, colocalization, pathway enrichment analysis, linkage disequilibrium score (LDSC) regression, and Mendelian Randomization (MR) analyses. Based on the identified genetic variants of NfL, we calculated polygenic risk scores (PRS) and assessed their association with the incidence of AD, and other AD-related endo-phenotypes using individual levels data from the Rotterdam Study cohort. In the current study, we identified two loci (*SLC39A11* and *UMOD*) in European and three loci (including *FMN2*) in African ancestry participants. Furthermore, we detected three loci (*FGGY, RN7SKP48*, and *TBX18*) in the trans-ethnic meta-analysis. PRS analyses based on European ancestry revealed significant associations with incident AD, and AD blood biomarkers (amyloid beta (Aβ)-40, Aβ-42, and total-tau). Moreover, our MR analysis demonstrated a potentially causal association between decreased kidney function and increased blood NfL levels.

Results
Our ancestry-specific GWAS meta-analysis of circulating levels of NfL was based on 11 different cohorts of European ($N = 18,532$) and three cohorts of African-American ancestry ($N = 1142$), Supplementary Table 1. The Rotterdam Study and the Rhineland study were the major contributors (>40%) to the total sample size. Participants of cohorts of European ancestry had diverse age ranges, varying from a mean age of 51 years (standard deviation [SD] = 3.2) in the Coronary Artery Risk Development in Young Adults (CARDIA) of European-American ancestry to a mean age of 85.3 years (SD = 6.7) in the Alzheimer's Disease Neuroimaging Initiative (ADNI) cohort. The female proportion varied from 0% in the Vietnam Era Twin Study of Aging (VESTA) cohort to 63% in the Cardiovascular Health Study (CHS) of European-American ancestry cohort. Among the three cohorts of African-American ancestry, the Atherosclerosis Risk in Communities (ARIC) cohort contributed the largest number of participants, while the Cardiovascular Health Study (CHS) participants were older (mean = 76.3 years [SD = 4.93]) compared to the other two cohorts (mean ages of 61.5 [SD = 4.5] and 48.9 [SD = 3.5] years in the ARIC and CARDIA cohort, respectively). Moreover, the CARDIA cohort of African-American ancestry had the lowest percentage of female participants (56.7%). Overall mean NfL levels in all participating cohorts were significantly positively correlated with mean age (Pearson's r = 0.81, $P = 2.06 \times 10^{-4}$).

GWAS meta-analysis findings
The European ancestry GWAS meta-analysis identified 26 genome-wide significant single nucleotide polymorphisms (SNPs) within two loci led by two individually significant SNPs (Supplementary Table 2). Manhattan plot and Quantile–Quantile (Q-Q) plot of the meta-analysis summary statistics are provided in Fig. 1A and Supplementary Fig. 1A. The first locus at 16p12 was mapped to the *UMOD* and *PDILT* genes, tagged by 39 SNPs with p values < 0.05 (Supplementary Data 1). This locus was led by two genetic variants reaching genome-wide significance, including rs7203642-A (effect = 0.041, standard error [SE] = 0.007, $P = 1.37 \times 10^{-8}$) in the intronic region of the *UMOD* gene and rs77924615-A (effect = −0.041, SE = 0.007,

$P = 3.77 \times 10^{-8}$) within the intronic region of the *PDILT* gene. A regional plot for the 16p12 locus (Fig. 2A) shows that both variants are also in high linkage disequilibrium (LD) with each other. Therefore, we defined this locus based on the rs7203642 variant of the *UMOD* gene, with the A-allele of rs7203642 associated with increased blood NfL levels. The second locus at chromosome 17q24 was tagged by 117 SNPs with a p value < 0.05 (Supplementary Data 1) and was mapped to the *SLC39A11* gene. At the 17q24 locus, the A-allele of the lead intronic variant rs12051560 (effect = 0.033, SE = 0.006, $P = 9.94 \times 10^{-9}$) was associated with increased blood NfL levels (Fig. 2B regional plot). The *UMOD* and *SLC39A11* signals were largely consistent throughout the cohorts included in the European ancestry based meta-analysis (Supplementary Fig. 2A, 3A). We also identified three additional suggestive loci (7p21, 10p12.1 and 12q24.22) at p values < 5 × 10^{-7} (Supplementary Data 2). One of these suggestive loci at 7p21 and tagged by an intergenic variant, was mapped to the *TMEM106B*, *VWDE* and *SCIN* genes (rs3902479-T; effect = 0.0303, SE = 0.059, $P = 3.05 \times 10^{-7}$) (regional plot is shown in Fig. 2C). Based on LSDC software, the SNP- heritability (h^2) of blood NfL levels was 0.12, meaning that the genotyped variants can explain about 12% of the variation of NfL levels in blood.

The Manhattan plot and Q-Q plots for GWAS meta-analysis of African-American ancestry are provided in Fig. 1B and Supplementary Fig. 1B. In the GWAS meta-analysis of African-American cohorts (Supplementary Table 2), we identified three independent genome-wide significant loci at chromosomes 1q43, 12q14, and 12q21 (Supplementary Data 3). An intronic variant inside the *FMN2* gene (rs1026417-C, effect = −0.433, SE = 0.076, $P = 1.36 \times 10^{-8}$) was associated with decreased levels of NfL in circulation, while two genetic variants at 12q14 (rs17098087-C, effect = 0.440, SE = 0.074, $P = 2.59 \times 10^{-9}$) and 12q21 (rs73423978-T, effect = 0.332, SE = 0.060, $P = 3.50 \times 10^{-8}$) were associated with increased levels of NfL in blood (regional plots shown in Fig. 3). There were 12 suggestive loci ($P < 5 \times 10^{-7}$) in African-American ancestry (Supplementary Data 2). We have provided information about Combined Annotation Dependent Depletion (CADD) score, Regulome Database (RDB) annotation, and chromatin state information for all SNPs inside the observed genetic loci for both European and African-American ancestry using the Functional Mapping and Annotation (FUMA) in Supplementary Data 1, 3–5 and Supplementary Figs. 2–6.

Trans-ethnic meta-analysis
In the trans-ethnic GWAS meta-analysis of European and African-American ancestry, we identified three loci showing evidence of association with plasma NfL levels at genome-wide significance (Supplementary Table 3). The Manhattan plot and Q-Q plots for trans-ethnic meta-analysis are provided in Fig. 1C and Supplementary Fig. 1C. The first locus, 1p32, was mapped to the *FGGY* gene led by rs11583796 ($P = 1.14 \times 10^{-10}$, $P_{ANS-HET} = 3.23 \times 10^{-12}$), and the second locus at 6q14 was found near the *TBX18* gene (rs58152294: $P = 1.95 \times 10^{-8}$, $P_{ANS-HET} = 1.05 \times 10^{-9}$). We identified 16 additional suggestive loci ($P < 5 \times 10^{-7}$), one of which (8p21) mapped to the *NEFM* gene ($P = 1.69 \times 10^{-7}$, $P_{ANS-HET} = 1.5 \times 10^{-4}$) (Supplementary Data 6 and Supplementary Fig. 7). SNPs identified in ancestry-specific meta-analysis were also observed in trans-ethnic meta-analysis including *FMN2* ($P = 3.08 \times 10^{-7}$, $P_{ANS-HET} = 3.32 \times 10^{-8}$), *UMOD* ($P = 2.25 \times 10^{-7}$, $P_{ANS-HET} = 0.122$), and *SLC39A11* ($P = 1.34 \times 10^{-7}$, $P_{ANS-HET} = 0.03891$). Annotation information of SNPs identified in trans-ethnic meta-analysis is provided in Supplementary Data 7 and 8.

Conditional analysis on kidney function and Alzheimer's disease
In the European ancestry meta-analysis, the locus at 16p12 (*UMOD* gene) is also a known locus for kidney function[12]. Kidney function was not included as a covariate in the GWAS of blood NfL levels by the participating cohorts, although it may have a role in blood protein clearance and thus may confound genetic associations of blood protein levels. To investigate whether genetic variants associated with kidney function may have confounded the associations between the identified SNPs and blood NfL levels, we conducted a conditional analysis by conditioning the observed genetic association effect size estimates on the estimated kidney glomerular filtration
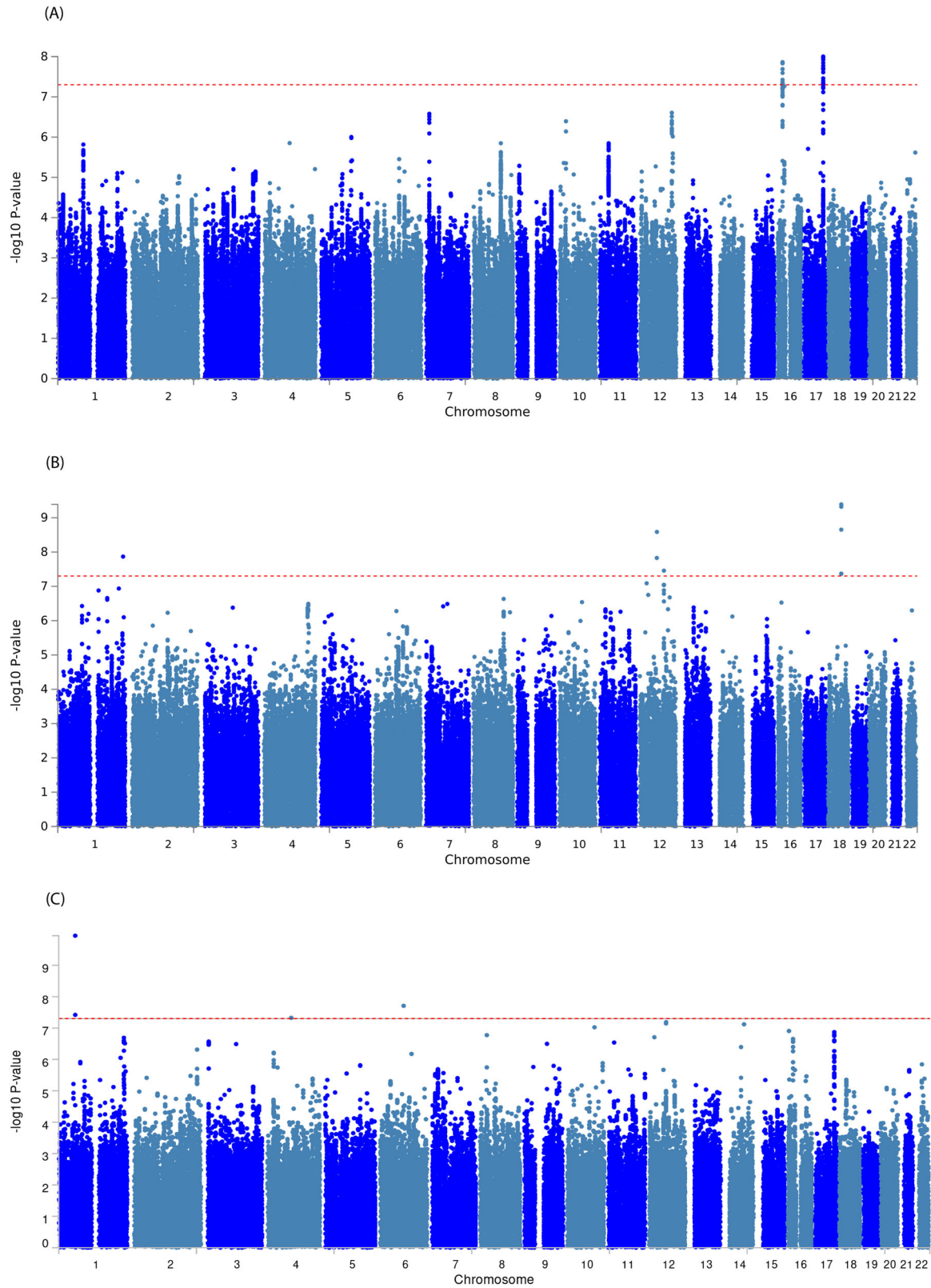
Fig. 1 | Manhattan plots for the meta-analysis of genome-wide association study (GWAS) of the blood levels of neurofilament light (NfL). Manhattan plot based on GWAS meta-analysis of the European ancestry (**A**), African- American ancestry (**B**), and Trans-ethnic participants (**C**). The Observed associations of all tested genetic variants on autosomal chromosomes (X-axis) are displayed as –log10(P values) on the Y-axis. The red dotted horizontal line indicates a genome-wide significant association (P value $< 5 \times 10^{-8}$) with NfL levels in blood.
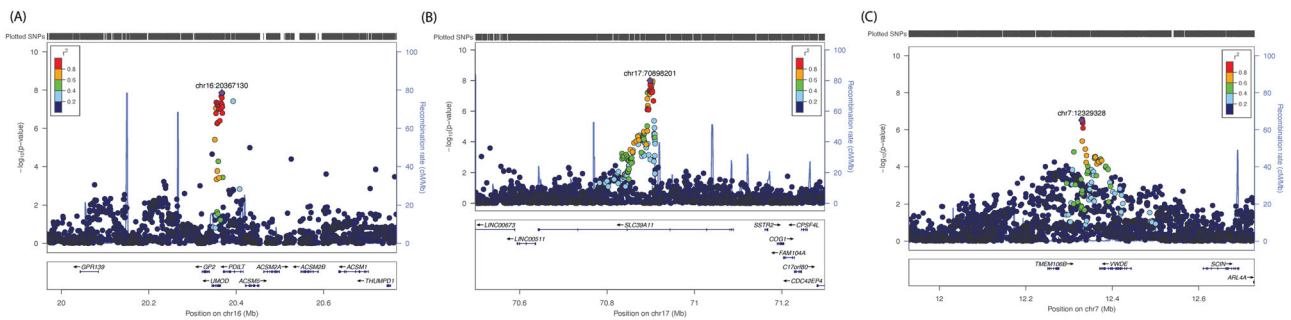
Fig. 2 | Loci identified in the European ancestry. Regional plot for two genome-wide significant loci in the *UMOD* (**A**), and *SLC39A11* (**B**), and suggestive locus near *TMEM106B/VWDE* genes (**C**) identified in the meta- analysis of neurofilament light (NfL) genome-wide association study (GWAS) in European ancestry. The genetic variants are denoted as colored circles with their *P values* (-log10) on left Y-axis and genomic location is based on build 37 on X-axis. Lead SNPs (purple diamond) are marked with their genomic location. Recombination rates are plotted on right Y-axis to represent the local linkage disequilibrium (LD) structure. The LD between the genetic variants is provided with a color scale, ranging from blue (r2 = 0) to red (r2 = 1). LD calculations are based on 1000 genome, European ancestry.
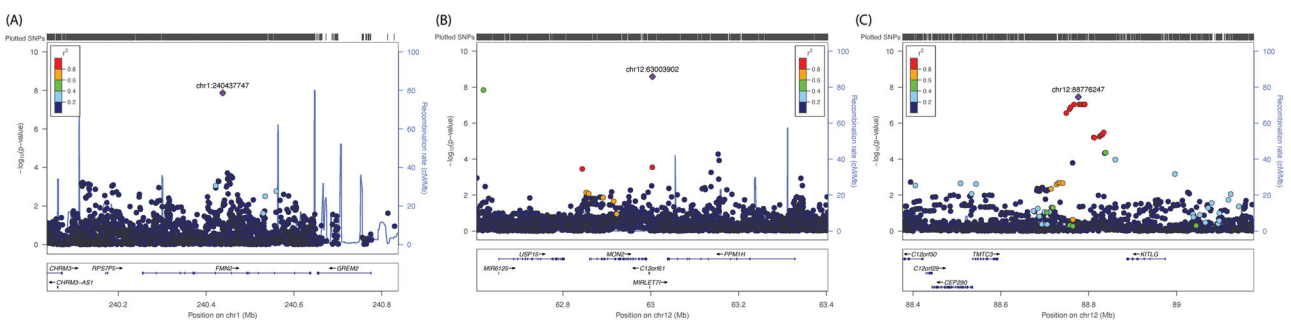
Fig. 3 | Loci identified in the African-American ancestry. Regional plot for three loci in *FMN2* (**A**), intergenic region at 12q14 (**B**) and 12q21 (**C**) identified in the meta-analysis of neurofilament light (NfL) genome-wide association study (GWAS) in African-American ancestry. The genetic variants are denoted as colored circles with their *P values* (-log10) on the left Y-axis and genomic location is based on build 37 on the X-axis. Lead SNPs (purple diamond) are marked with their genomic location. Recombination rates are plotted on right Y-axis to represent the local linkage disequilibrium (LD) structure. The LD between the genetic variants is provided with a color scale, ranging from blue (r2 = 0) to red (r2 = 1). LD calculations are based on 1000 genome, African ancestry.

rate (eGFR)[12] associated genetic variants in European ancestry using mtCOJO[13]. Results of this conditional analysis showed that one of the lead genetic variants at 17q24 (rs12051560-A, Effect = 0.033, SE = 0.006, $P = 9.13 \times 10^{-9}$) is independent of kidney function (Supplementary Data 9). However, the second variant inside the intronic region of *UMOD* gene became less significant (rs7203642-A, effect = 0.034, SE = 0.007, $P = 3.51 \times 10^{-6}$) upon conditioning the meta-analysis on kidney function. Since some of the participating cohorts included in the meta-analysis also included AD patients, we also conditioned the observed effect size estimates of blood NfL levels in European ancestry meta-analysis on AD[18] associated genetic variants using mtCOJO (Supplementary Data 9). Results showed that both top genetic loci remained significant after adjusting the summary statistics of NfL levels in European ancestry for AD associated variants (rs12051560-A, Effect = 0.034, SE = 0.006, $P = 7.75 \times 10^{-9}$; rs7203642-A, effect = −0.041, SE = 0.007, $P = 1.69 \times 10^{-8}$).

Gene enrichment analysis

Gene enrichment analysis of both European (number of genes = 18,718) and African- American (number of genes = 17,370) ancestry-based meta-analysis showed enrichment of several Gene Ontology (GO) terms, though they did not pass the Bonferroni-adjusted thresholds for multiple testing (Supplementary Data 10). We also did not find an overlap in the top ten curated GO terms in the ancestry-specific enrichment analysis. Yet, the top GO terms enriched in European ancestry meta-analysis included GO molecular function beta-2 adrenergic receptor binding ($P = 1.89 \times 10^{-5}$), GO biological process glycerolipid catabolic process ($P = 2.97 \times 10^{-5}$), germ cell pro-liferation ($P = 6.85 \times 10^{-5}$), and canonical wnt signaling pathway ($P = 5.57 \times 10^{-5}$). In addition, genes were enriched in curated gene sets

including sharma pilocytic astrocytoma location dn, reactome foxo medi-ated transcription of cell death genes, and pid p38 alpha beta downstream pathway. In African-America ancestry meta-analysis findings were enri-ched for GO biological process astrocyte differentiation ($P = 1.38 \times 10^{-4}$), compartment pattern specification ($P = 1.85 \times 10^{-4}$) and GO astrocyte development ($P = 9.38 \times 10^{-4}$). In the trans-ethnic meta-analysis, we iden-tified significant association of GO term CUL3 Ring Ubiquiti ligase complex ($P = 1.66 \times 10^{-6}$). We also observed enrichment of GO biological process neurofilament cytoskeleton organization ($P = 1.25 \times 10^{-4}$), but this asso-ciation was not significant after Bonferroni correction.

eQTL analysis for the identified genetic variants

The eQTL analysis findings related to SNPs located within genome-wide significant and suggestive loci in the European, African-American, and the trans-ethnic ancestry are presented in Supplementary Data tables 1, 4, 5, 8. Notably, the effect allele of the lead genetic variant on chromosome 17, rs12051560-A, was associated with decreased expression of the *SSTR2* gene in cerebellar hemispheres (Normalized Effect Size [NES] = -0.28, $P = 1.66 \times 10^{-7}$) and the cerebellum (NES = –0.26, $P = 7.20 \times 10^{-6}$). Multiple suggestive loci at 7p21 in European ancestry showed significant association with the expression of the *VWDE* gene in various brain tissues (Supple-mentary Data 4). In the trans-ethnic meta-analysis, seven intergenic SNPs within suggestive loci (near *NEFM*) also acted as eQTL for the expression levels of the *NEFM* gene in the basal ganglia (Supplementary Data 8)

Genetic correlation of NfL with neurological traits

In the LD regression analysis based on the results of European ancestry meta-analysis (Supplementary Data 11), we observed no genetic correlation
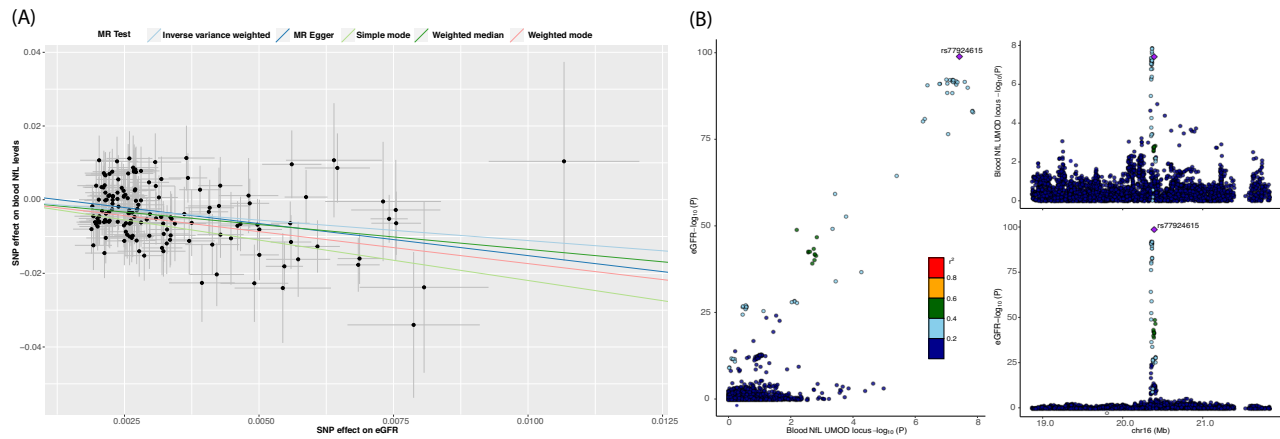
Fig. 4 | Mendelian Randomization and Colocalization analysis. Scatter plot of instrumental variable (SNPs) effect size estimates of kidney function (eGFR) on NfL in two sample Mendelian Randomization analysis (**A**), and Colocalization plot between *UMOD* locus and eGFR (kidney function) in European ancestry (**B**).

with any neurological or neurology-derived traits. The genetic correlation coefficients were in positive direction for AD, T-tau, Aβ-40, Aβ-42, and Aβ-ratio. As a sensitivity test, we also repeated the LD regression analysis using the European ancestry NfL summary statistics conditioned on kidney function (Supplementary Data 11), but the results remained similar to the original unadjusted summary statistics. Furthermore, colocalization analysis of two loci in individuals of European ancestry did not demonstrate a significant posterior probability of colocalization with neurological traits (Supplementary Data 12).

Polygenic risk score analysis in the Rotterdam Study
We further corroborated the results of the LD regression analyses, which were based on summary statistics, by deriving a PRS based on individual-level data (Supplementary Data 13). In the Rotterdam Study cohort, the PRS based genome-wide significant threshold (PRS $_{Threshold}$ = 5×10^{-8}) in European ancestry participants showed strong associations with plasma levels of total tau (effect size = 0.836, False discovery rate (FDR) = 6.81×10^{-4}), Aβ-40 (effect size = 0.550, FDR = 1.24×10^{-4}), and Aβ-42 (effect size = 0.638, FDR = 9.33×10^{-4}). Association analysis of PRS score based on higher p value thresholds (PRS $_{Threshold}$ 1.0×10^{-4}; FDR = 1.50×10^{-3}; PRS $_{Threshold}$ 0.001; FDR = 1.60×10^{-3}; PRS $_{Threshold}$ 0.05; FDR = 2.32×10^{-5}) showed significant association with AD incidence, as well as with imaging phenotypes including total brain volume (PRS $_{Threshold}$ 1×10^{-6}; FDR = 3.30×10^{-2}), and total white matter lesions (PRS $_{Threshold}$ 0.05; FDR = 1.34×10^{-3}).

Relation of identified single genetic variants with neurological traits
We also performed look-ups of the two identified genetic variants associated with blood NfL levels in European ancestry participants using AD[14,15], PD, and other GWAS (meta-analysis) summary statistics included in our LD regression analyses (Supplementary Data 14).

Neither of the two genetic variants showed an association with AD or PD. The genetic variant inside *UMOD* (rs7203642-A) gene showed weak evidence of association (Bonferroni correction [0.05/12] <4.16×10^{-3}) with Aβ-40 (β = 0.039, P = 1.37×10^{-2}), Aβ-42 (β = 0.033, P = 4.43×10^{-2}) and significant association with total-tau (β = 0.028, P = 6.21×10^{-4}). The associations of the variant within the *SLC39A11* gene (rs12051560-A) with total-tau (β = 0.012, P = 7.30×10^{-2}) and total brain volume (P = 3.25×10^{-2}) were not significant after multiple testing correction. Of the single genetic variants associated with blood NfL levels, which were assessed in relation to CSF levels of Aβ-42, phosphorylated tau (p-tau), total-tau in the MEMENTO cohort (Supplementary Data 15), only one genetic variant rs12051560-A (*SLC39A11*) was related to CSF levels of total tau (β = 0.138, P = 4.96×10^{-2}).

Two-sample MR
In the forward MR (the effect of kidney function on blood NfL levels) analysis, we observed a potential causal association between kidney function and blood NfL levels based on the inverse variance weighted (IVW) method (β = –1.045, P = 6.19×10^{-8}). MR estimates from other robust methods also showed consistent results, including MR-Egger (β = –1.912, P = 1.29×10^{-4}), weighted median (β = –1.32, P = 4.31×10^{-7}), simple mode (β = –2.13, P = 6.84×10^{-3}), and weighted mode (β = –1.75, P = 5.73×10^{-3}) (Supplementary Data 16). However, the significant Cochran Q statistic for inverse variance weighted method (P = 7.0×10^{-4}) and the MR-Egger method (P = 3.98×10^{-4}) indicated heterogeneity in our MR estimates. No evidence of directional horizontal pleiotropy was observed based on the Egger intercept of 0.003 (p value = 0.054). Among the 168 instrumental variables, we identified 15 outliers using the radial MR method that contributed to the significant heterogeneity. Sensitivity analysis after excluding the outliers from the instrumental variables showed consistent significant results among all MR methods (Fig. 4A) with no evidence of heterogeneity or horizontal pleiotropy in estimates (Q-P_{IVW} = 0.733 and Q-$P_{MR-Egger}$ = 0.709, $P_{Egger\ intercept}$ = 0.147). MR-PRESSO results also showed significant MR estimates after removal of outliers (β = –0.977, P = 1.19×10^{-7}). In the reverse MR (the effect of blood NfL levels on kidney function), we did not find evidence for causality based on the inverse variance weighted MR method (β = –0.104, P = 1.02×10^{-1}).

Colocalization analysis between NfL loci and kidney function in European ancestry
Colocalization analysis revealed that the NfL locus within the *UMOD* gene and kidney function (eGFR) share a single causal variant with posterior probabilities of the single shared causal variant (PP:H4) > 0.819 (Fig. 4B, Supplementary Data 12), whereas the other locus near *SLC39A11* showed no evidence of colocalization of causal variants between both traits (PP H4: 1.21×10^{-4}) (Supplementary Fig. 8).

Discussion
In the ancestry-specific GWAS meta-analyses, we identified two genome-wide significant loci (16p12 and 17q24) associated with blood NfL levels within the *UMOD* and *SLC39A11* genes, and three suggestive loci, one (7p21) mapped to the *TMEM106B* gene, among European ancestry participants. Additionally, we identified three genome-wide significant loci (1q43, 12q14, and 12q21) in participants from the African-American ancestry. Further, in the trans-ethnic meta-analysis, we identified three more loci (1p32, 4q21, 6q14) mapped to the *FGGY*, *RN7SKP48*, *TBX18* genes, and 16 suggestive loci, one (8p21) located near to the *NEFM* gene. Evaluation of the genetic correlation of the blood NfL levels (European ancestry) with neurological traits demonstrated no significant genetic

correlation. However, a PRS based on European ancestry was associated with plasma levels of Aβ-42, Aβ-40, total-tau, and the incidence of AD in the Rotterdam Study cohort. MR and colocalization analyses demonstrated evidence for a causal association between lower kidney function and higher blood NfL levels in European ancestry.

The locus at 17q24 (*SLC39A11*) was associated with blood NfL levels at the genome-wide level of significance in European ancestry. Several lines of evidence from earlier studies indicate the role of the *SLC39A11* gene in neurodegeneration. The *SLC39A11* gene plays a role in zinc homeostasis[16] and has been associated with ALS[17,18] ($P = 8.11 \times 10^{-6}$). The KEGG pathway database (map05010 and map05012) queries indicated a role of the *SLC39A11* gene in the AD- as well as PD-related pathways[19]. The *SLC39A11* gene is expressed in the brain based on data from the human protein atlas[20] and the genotype-tissue expression (GTEx) database, but apart from the *SLC39A11* variants (Supplementary Data 1) that acted as an eQTL for the *SSTR2* gene in cerebellar tissue, no other variants in *UMOD* locus were identified as eQTLs in the GTEx database. Another interesting observation that links the *SLC39A11* polymorphisms to neuro-axonal injury is that the rs12051560-A (*SLC39A11*) associated with decreased expression of the somatostatin receptor 2 (*SSTR2*) gene in the cerebellum and the cerebellar hemispheres based on the queries of the GTEx eQTL database. Decreased expression of *SSTR2* gene was linked to axonal degeneration of noradrenergic projections in *SSTR2–/–* mice studies[21]. Earlier studies also implicate the *SSTR2* gene in neurodegeneration under ischemia[22], and in hypoxia-induced neuronal cell death[23].

Another locus for blood NfL levels in European ancestry participants was identified in the 16p12.3 region, which is tagged by two lead genetic variants located inside the *UMOD* and *PDILT* genes, which have previously been associated with kidney function[12]. Conditional analysis on kidney function showed that the association of our lead SNP rs7203642 became less significant ($P = 3.51 \times 10^{-6}$). The *UMOD* findings are in line with results from earlier studies reporting an association between decreased kidney function and increased blood NfL levels, which may be due to aging, cardiovascular risk factors, and diabetes mellitus[24-27]. The observation of higher blood levels of NfL in children with chronic kidney disease[28] contradicts the role of cardiovascular diseases and diabetes as the sole drivers of blood NfL levels. Nevertheless, kidney function has been associated with cognitive decline, brain atrophy, and white matter abnormalities[29,30] which suggest a direct role of kidney function in determining blood NfL levels. Our MR analysis robustly demonstrated a potential causal relationship between decreased kidney function and increased blood NfL levels, which remained consistent across different MR methods. Among the two loci identified in European ancestry (*UMOD* and *SLC39A11*), only the *UMOD* locus exhibited significant colocalization with kidney function (eGFR), reinforcing the *UMOD* gene's role as a shared genetic driver of blood NfL levels and kidney function. The exact mechanism through which genetic variants in the *UMOD* and blood levels of NfL are related requires further investigation. However, the key role of *UMOD* in kidney function may be instrumental in understanding its link to neurodegeneration. The *UMOD* gene encodes for the uromodulin protein and mutations in this gene have been associated with hyperuricemia and tubulointerstitial nephritis[31]. One of the primary reasons for *UMOD*-related kidney disease is the accumulation of misfolded *UMOD* protein inside the endoplasmic reticulum (ER)[32] and thereby generation of ER stress which results in cell death and inflammation[33]. Hyperglycemia and ER stress related pathways may trigger the generation of advanced glycation end products (AGE), which have been associated with neurodegeneration[33,34]. Second, the lead genetic variants of identified locus (i.e., rs77924615) was found inside the *PDILT* gene, which belongs to the protein-disulfide isomerase (PDI) family of proteins[35]. PDI proteins play an important role in protein folding in the ER and their dysfunction may lead to diseases involving the accumulation of misfolded proteins, which is also a hallmark of neurodegenerative diseases such as AD and PD[12].

One of the suggestive loci of blood NfL levels in European ancestry meta-analysis was located near the *TMEM106B* gene, which is known to influence CSF NfL levels[11]. The identification of a common gene influencing NfL levels in both blood and CSF aligns with the reported correlation between plasma and CSF NfL levels[36]. An early reported protein quantitative trait locus (pQTL) of the TMEM106B protein[37] (rs1548884-C, effect size = −0.26, SE = 0.019, $P = 7.23e-42$) also showed an association with blood NfL levels in our meta-analysis (rs1548884-C, effect size = −0.0209, SE = 0.0068, $P = 3.34 \times 10^{-4}$), suggesting genetic pleiotropy or shared biological pathways that warrants further investigation. To gain further insight, we performed a two-sample MR analysis to evaluate the causal association between blood TMEM106B and NfL levels, which showed a significant link between increased TMEM106B protein levels with increased NfL levels (wald ratio: effect size = 0.08, $P = 3.14 \times 10^{-4}$). The *TMEM106B* gene is a known locus for neurodegenerative diseases, with reported implications in sites of onset, motor functions, and cognition in ALS[38] and AD[39]. It also acts as a modifier of frontotemporal dementia (FTD) risk[40]. Moreover, the *TMEM106B* gene contributes to the pathophysiology of frontotemporal lobar degeneration (FTLD) by interacting with the progranulin protein and altering lysosomal activity[41].

We identified a locus in the trans-ethnic meta-analysis in the *FGGY* gene, which has been previously associated with sporadic ALS[42,43], but was not replicated in subsequent studies[44]. In our meta-analysis, the direction of the association was not consistent across different cohorts and the lead SNP showed highly significant ancestral heterogeneity ($P = 3.23 \times 10^{-12}$). The *FGGY* gene codes for a family of carbohydrate kinases[45], which have a role in energy metabolism and glycolysis[46]. The identification of the *FGGY* locus is relevant due to the importance of NfL levels as specific markers of ALS disease progression and survival[47].

We also identified a suggestive association of blood NfL levels with a locus mapped to the *NEFM* gene, which encodes the neurofilament medium chain protein that plays a role in axonal radial growth and stability of neurofilament network[48]. The direction of effect size estimates of the lead variant (rs196876) was consistent over all 14 cohorts from two ethnicities, which makes this locus a plausible target for future investigations. This locus is also supported by the observation that 7 SNPs within the locus have shown association (eQTLs) with *NFEM* expression in the basal ganglia (Supplementary Data 8). The GTEx database showed expression of *NEFM* predominantly in brain tissues and earlier studies have reported the association of *NEFM* expression dysregulation with ALS[49]. An earlier study also linked a point mutation within the *NEFM* gene to early onset PD[50], which did not emerge in large genetic studies.

NfL PRS at the genome-wide significant threshold was associated with plasma levels of t-tau, Aβ-40, and Aβ-42 in the Rotterdam Study. Notably, PRS analyses constructed using more lenient p value thresholds (i.e., 1×10^{-4}, 1×10^{-3}, and 0.05) were significantly associated with the incidence of AD. Although single SNP lookups and genetic correlation analyses using summary-level data did not show associations between NfL and Aβ-40 or Aβ-42, the association of PRS at different p value thresholds suggest a shared biological mechanism underlying these core AD biomarkers. Additionally, the broader set of NfL-associated variants better captured AD risk, potentially indicating the presence of neurodegeneration related loci that did not reach genome-wide significance in the meta-analysis such as *TMEM106B*. PRS based association findings, together with the observed association of the variant inside the *UMOD* gene ($P = 6.21 \times 10^{-4}$) with blood total-tau levels, supports the notion that genetic determinants of blood NfL levels are likely linked to central neurodegeneration.

In the participants from the African-American ancestry, one of the three loci was located near the *FMN2* gene (rs1026417-C). *FMN2* is a coding gene involved in the cytoskeleton assembly, which makes it an important discovery since NfL is a cytoskeleton protein released into extracellular space as a result of neuro-axonal damage[7]. *FMN2* gene is highly expressed in the brain and involved in synaptic plasticity and memory formation[51]. Our observation was concordant with several studies that reported the association of the *FMN2* gene with cognition[52], ALS[53], intellectual development disorder[54] and neuropsychiatry traits[55]. All these interlinked pieces of evidence support the role of the *FMN2* gene in determining the blood NfL levels in various neurological diseases in African-American ancestry. None

of the genetic variants identified in the African-American ancestry meta-analysis showed association with blood NfL levels in the European ancestry.

Next, in the pathway-enrichment analysis based on the European ancestry, we did not identify significant enrichment of GO biological processes for our observed genes after multiple testing correction. However, GO: canonical wnt signaling pathway ($P = 5.57 \times 10^{-5}$) and GO: regulation of wnt signaling pathway ($P = 1.43 \times 10^{-4}$) were among the top pathways that were enriched for 307 and 334, respectively, of the putative genes identified in our study. Wnt signaling is one of the most crucial pathways involved in brain development and involves several genes associated with neurodegenerative diseases such as AD and PD[56]. Furthermore, the 'beta 2 adrenergic receptor' binding GO molecular process ranked first in our analysis ($P = 1.89 \times 10^{-5}$). Interestingly, blocking the beta 2 adrenergic receptors is found to be an effective approach in PD to reduce neuroinflammation and degeneration of dopaminergic neurons[57,58]. In the African-American ancestry, in GO biological processes, astrocyte differentiation ($P = 1.38 \times 10^{-4}$) and astrocyte development ($P = 3.38 \times 10^{-4}$) were the most notable terms enriched in the GWAS, which reiterates the role of astrocytes in neurodegeneration[59]. In the trans-ethnic pathway-enrichment analysis, GO cellular component term CUL3 ring ubiquitin ligase complex emerged, which has been linked to regulation of neurofilaments[60,61]. GO biological process neurofilament cytoskeleton organization ($P = 1.25 \times 10^{-4}$) showed enrichment for 8 genes.

Our study represents the largest GWAS to uncover the genetic determinants of NfL levels in blood. Our GWAS sample included 11 different cohorts of both European and African-American ancestry, which is also the main strength of our study. The genetic variant inside *UMOD* gene (rs7203642) identified in our study not only highlight the importance of kidney function in neurodegeneration but also indicates that kidney function should be taken into account when assessing blood-based protein biomarkers and specifically NfL. This study has also limitations. A few participating cohorts also included AD patients in the GWAS. Although, we adjusted the analyses for case-control status, and also performed a conditional analysis based on European GWAS meta-analysis summary statistics, a more sensitive approach would be to consider a stratified GWAS based on a dementia-free population for future NfL GWAS. The small sample size of African-American cohorts was a major limitation of the trans-ethnic meta-analysis.

In conclusion, we identified two unique loci associated with blood NfL levels in participants from European ancestry, three loci in African, and three unique loci in a trans-ethnic meta-analysis. Further, we validated a known locus (near *TMEM106B* gene) of CSF NfL levels, which is also implicated in ALS, FTD, and AD. Our findings highlight the role of the *UMOD* gene in linking reduced kidney function to increased blood NfL levels.

Methods
Study populations
The current study includes 18532 participants of European and 1142 participants of African-American ancestry from 11 different cohorts of the CHARGE consortium including: the Rotterdam Study (RS-I and RS-II, $N = 4119$), the Rhineland Study ($N = 4019$), the MEMENTO cohort ($N = 2195$), the Framingham Heart Study (FHS, $N = 2048$), the BiDirect study ($N = 1899$), the CHS (African-American $N = 273$, European-American $N = 1396$), the ARIC (African-American $N = 823$, European American $N = 742$), the VESTA ($N = 828$), the ADNI ($N = 578$), the CARDIA (African-American $N = 128$, European-American $N = 343$) Study, and the Austrian Stroke Prevention Family Study (ASPS-Fam, $N = 287$). Prior to participation, each participant gave written, informed consent. A detailed description of each of the participating cohorts, their genotyping information, and the quantification of NfL is described in the supplementary materials. General demographic information is provided in Supplementary Table 1.

NfL quantification
Different protocols were adopted by participating cohorts for sample preparation, plasma or serum extraction, and NfL quantification.

Methodological details concerning NfL quantification are provided in the cohort descriptions included in the supplement (Supplementary Data 17). In summary, the Rotterdam Study used the single molecule array (Simoa) HD-1 analyzer platform, the Rhineland study used the Quanterix Simoa NF-light assay (103186), the FHS, ARIC, and CARDIA cohorts used the Quanterix 4-Plex, the MEMENTO cohort used Simoa NF-light kit on a Quanterix H1 analyzer, BiDirect Study profiled NFL on Simoa HDX analyzer, ADNI cohort used simoa HD-1 analyzer, VESTA cohort used single analyte assays using the Quanterix Simoa HD-1 platform, CHS used the Simoa Human Neurology 4-Plex A assay and the ASPS-fam used Simoa HDX analyzer.

Genotyping and imputation
The participating cohorts genotyped their samples employing various genotyping kits and imputed using either 1000 Genomes (1Kg)[62] or the Haplotype Reference Consortium (HRC)[63] panels. Detailed descriptions of the genotyping and imputation methods are provided in cohort description (Supplementary Data 17).

GWAS
Each participating cohort performed genome-wide association of SNP and plasma or serum levels of NfL using an additive model. Blood levels of NfL were log2 transformed before conducting the GWAS and analyses were adjusted for age, sex, study-specific covariates (including batch, study sites, case-control status (if applicable)), and genetic principal components to account for population structure and family relatedness. A post-GWAS quality control was performed on summary statistics of each study using the EasyQC software[64]. We excluded SNVs with low imputation quality scores (INFO score or $r^2 < 0.3$), low frequency (minor allele count <5 or minor allele frequency < 0.01), and variants that were available in less than 30 participants for each cohort. In order to identify ancestry-specific genetic variants, we performed an ancestry-stratified GWAS meta-analysis for three cohorts of African-American ancestry and 11 cohorts of European ancestry separately, using METAL[65] with inverse variance weighted average score to account for population heterogeneity and genomic inflation. In the European ancestry GWAS meta-analysis, we retained only 7,058,703 (~7 million) genetic variants that were present in at least two major cohorts (i.e., the Rotterdam Study and the Rhineland Study) of a total of 11 cohorts accounting for more than 40% of the total number of European ancestry participants. We also performed conditional analysis using GCTA mtCOJO[13] to identify genome-wide significant variants independent of kidney function[12] and Alzheimer's disease[14]. Due to sample sizes of the three participating African-American ancestry, we only retained 8,381,611 (~8 million) genetic variants that were present in all three cohorts of African ancestry (i.e., ARIC-AA, CHS-AA, and CARDIA-AA). Moreover, we excluded variants with heterogeneity I^2 values greater than 0.75 in the ancestry-specific meta-analysis. To perform the trans-ethnic meta-analysis based on European and African-American based GWAS summary data, we used MR-MEGA[66] software (--pc 12), where we corrected the results of each cohort for genomic inflation. We only retained SNPs present in three large European cohorts (Rotterdam Study I, II and Rhineland study) as well as in three African-American cohorts (4,833,685 SNPs). We also filtered out variants with significant residual heterogeneity ($P < 5 \times 10^{-8}$).

Functional mapping and annotation
To perform functional mapping, and annotation of GWAS summary statistics of NfL, we used the FUMA platform version 1.3.8 which is designed to prioritize and aid in the interpretation of GWAS findings[67,68]. To identify independent genome-wide significant SNPs, we used $r^2 = 0.2$ and P value $< 5 \times 10^{-8}$. Using FUMA, we defined the lead SNPs as independent of each other at $r2 = 0.1$ within a 500 kb region in the 1000

Genome Phase 3 reference panel. The individual lead SNPs were mapped based on the default 10 kb distance between SNPs and genes. The ancestry-specific GWAS and trans-ethnic GWAS meta-analysis NfL loci were visualized using Manhattan plots and regional plots using FUMA and Locus Zoom[69] (using the 1000 Genomes reference panel for estimating LD), respectively. We used LD score (LDSC) regression software[70] to estimate blood NfL heritability based on GWAS summary statistics. Reference LD scores were computed based on the 1000 Genomes Phase 3 reference panel.

Pathway enrichment analysis and functional analysis

Gene-based and gene-set enrichment analyses, which quantify the association of individual mapped genes with NfL levels and sets of genes with GO terms, respectively, were performed using MAGMA (version v1.0.8)[71] as implemented in FUMA (version 1.3.7). The gene-based analysis was performed based on 18,718 protein-coding genes, setting the level of statistical significance at a Bonferroni-adjusted threshold of P value = 2.671×10^{-6} (= 0.05/18718). For MAGMA gene-set analysis, gene-set p value is computed using the gene-based P value for 4728 curated gene sets (including canonical pathways) and 6,166 GO terms obtained from MsigDB v5.2, and a FDR was used to correct for multiple testing.

Similarly, tissue-specific gene expression analysis was also performed using MAGMA as integrated in FUMA. Further, we explored the effects of genetic variants identified in our GWAS on the expression levels of other genes by querying the GTEx[72] database (version 8) for all SNPs included in identified loci using FUMA (in blood and brain tissue). Functional consequences for the SNPs were obtained by querying different databases, including ANNOVAR categories, CADD scores and RegulomeDB scores. ANNOVAR annotates the functional consequences of SNPs on genes (for example, intron, exon, and intergenic). CADD scores predict how deleterious the effect of a SNP may be, with scores above the 12.37 threshold flagged as potentially pathogenic. The RegulomeDB score is a categorical score based on information from eQTLs and chromatin marks, ranging from 1a to 7, with lower scores indicating an increased likelihood of having a regulatory function.

LD score regression analysis

To quantify the genetic correlation between blood NfL levels and other neurological traits and

biomarkers of neurodegeneration, we performed LD regression analysis. We obtained GWAS summary statistics for AD[14,39], PD[15], Huntington's disease[73], ALS[74], Aβ-42, Aβ-40[75], total-tau[76], and brain imaging markers (total hippocampal volume[77], total brain volume[78], and total white matter lesions[79]) from the GWAS catalog[80]. We performed LD score regression analysis using the LDSC tool[70] based on the European ancestry 1000 Genomes (phase 3) LD reference panel. Details of the GWAS studies used for LD regression and their base heritability estimates are provided in Supplementary Data 18.

PRS association with AD biomarkers

We calculated PRS based on NfL associated SNPs applying different p value thresholds (i.e., 5×10^{-8}, 1×10^{-7}, 1×10^{-6}, 1×10^{-5}, 1×10^{-4}, 1×10^{-3}, and 0.05) using PRSice-2[81]. PRS was calculated in the Rotterdam Study participants by summing the number of effect alleles weighted by their effect size estimates obtained from our meta-analysis based on European ancestry. In the PRS calculation, we retained variants with MAF > 0.01 in the target population and performed clumping using an r^2 value of 0.1. We used the Cox-proportional-hazard models to check the association of PRS with the incidence of AD, adjusted for age at baseline and sex. Moreover, we performed multiple linear regression analyses to assess the association of NfL PRS with plasma levels of Aβ-40, Aβ-42, Aβ-40/Aβ-42 ratio, total tau, as well as with magnetic resonance imaging (MRI) markers of neurodegeneration including total hippocampal volume, total brain volume, and total white matter lesions in the Rotterdam Study cohort. All linear regression analyses

were adjusted for age, sex, batch (in case of biomarkers), and additionally for intracranial volume for MRI traits.

Look up of lead variants into previous GWASs of neurological traits

To evaluate the association of the most significant genetic variants with the two common neurodegenerative diseases AD and PD, we used the most recent GWAS meta-analyses of AD[14] and PD[15] and reported the results for each genetic variant. Additionally, we performed lookups for single variants in GWASs of traits used for LD regression analysis. Bonferroni correction was used for multiple comparisons adjustment.

Colocalization analysis

We performed colocalization analysis to evaluate whether the loci discovered in the European ancestry meta-analysis are colocalized with neurological traits considered for lookups. The variants within ±1.5 megabases (Mb) of the lead SNPs in European ancestry were used for the colocalization analysis. We utilized the 'coloc.abf ' function from the COLOC[82] R package to test the posterior probabilities (PP) between SNPs associated with NfL and various phenotypes under the following hypotheses: (PP:H0) neither trait has a genetic association in the region; (PP:H1/PP:H2) only one trait has a genetic association in the region; (PP:H3) both traits are associated but with different causal variants; and (PP:H4) both traits are associated and share a single causal variant. The prior probability for H4, set at 1.0×10^{-6}, was used to determine the likelihood that a random variant is causative for both NfL and the tested phenotypes. We used locusComparer[83] R package to visualize the colocalization results.

Mendelian Randomization

To evaluate the causality of the association between kidney function and blood NfL levels in individuals of European ancestry, we performed two-sample MR analysis using the TwosampleMR[84] package. We used inverse-variance weighted regression as the primary MR method, followed by other complementary methods robust to instrumental variable bias due to horizontal pleiotropy, including weighted median[85] and MR-Egger[86] regression. Exposure instrumental variables were defined as genome-wide significant ($P < 5 \times 10^{-8}$), independent ($r^2 = 0.001$) within a window of 10,000 kb. To assess the robustness of our MR results to various assumptions related to instrumental variables, we performed several sensitivity analyses, including (i) the Cochran Q statistics to estimate the pleiotropy of causal estimates, (ii) MR-Egger intercept to identify horizontal pleiotropy, and (iii) radial MR[87] and MR-PRESSO to detect outliers in instrumental variables and MR estimates after removing outliers, respectively. Finally, we performed a reverse MR to exclude the possibility of reverse causation.

Statistics and reproducibility

Baseline characteristics of each cohort were assessed and summarized in Supplementary Table 1. Statistical and genetic analyses were conducted using various command line tools including EasyQC[64], Plink 1.9 (version 1.9, https://www.coggenomics.org/plink/), and R (version 4.0.4, https://www.r-project.org/) statistical environment. Meta-analysis of GWAS summary statistics was performed using METAL[65] software (latest version released on 2011-3-25, https://csg.sph.umich.edu/abecasis/metal/download/) and MR-MEGA (version 0.2, https://genomics.ut.ee/en/tools). We used the web-based tool FUMA[67] (version 1.3.8 and 1.5.2, https://fuma.ctglab. nl/) to perform LD pruning, lead loci detection, eQTL (GTEX v8, https://gtexportal. org/home/) analysis, and other functional analyses. Locuzoom was used to plot regional plots for genetic loci (http://locuszoom.org/). For PRS calculation, we used PRSice-2 (version v2.3.3, https://github.com/choishingwan/ PRSice) software while MR and colocalization analyses were performed using TwoSampleMR (version 0.5.7, (https://mrcieu.github.io/TwoSampleMR/ articles/introduction.html) and coloc (version 5.2.3, https://github.com/ chr1swallace/coloc) R packages. Details of tools used by each participating cohort for performing GWAS are provided in supplementary Data 17.

Reporting summary

Further information on research design is available in the Nature Portfolio Reporting Summary linked to this article.

Data availability

All data generated during this study are included in this published article and its supplementary information/data files. Summary statistics of the GWAS is made available publicly in GWAS catalog (GCP000993). We used publicly available data in this manuscript, including data from GTEx version 8 (https://gtexportal.org/home/) and publicly available GWAS summary statistics for total hippocampal volume (https://www.ebi.ac.uk/gwas/publications/30279459), total brain volume (https://www.nature.com/articles/s41588-019-0516-6#Sec22), Alzheimer's disease (https://www.ebi.ac.uk/gwas/publications/30820047, https://www.ebi.ac.uk/gwas/publications/35379992), Parkinson's disease (https://www.ebi.ac.uk/gwas/studies/GCST90043734, https://www.ebi.ac.uk/gwas/studies/GCST009324), white matter lesions (https://www.ebi.ac.uk/gwas/publications/33293549), t-tau (https://www.ebi.ac.uk/gwas/publications/35396452), amyotrophic lateral sclerosis (https://www.projectmine.com/research/download-data/), Huntington's disease (https://datadryad.org/stash/dataset/doi:10.5061%2Fdryad.5d4s2r8), amyloid beta 40, 42 and ratio (https://alz-journals.onlinelibrary.wiley.com/doi/epdf/10.1002/alz.12333).

References

1. Gaetani, L. et al. Neurofilament light chain as a biomarker in neurological disorders. *J. Neurol. Neurosurg. Psychiatry* **90**, 870–881 (2019).
2. Zetterberg, H. Neurofilament light: A dynamic cross-disease fluid biomarker for neurodegeneration. *Neuron* **91**, 1–3 (2016).
3. Disanto, G. et al. Serum Neurofilament light: A biomarker of neuronal damage in multiple sclerosis. *Ann. Neurol.* **81**, 857–870 (2017).
4. Khalil, M. et al. Serum neurofilament light levels in normal aging and their association with morphologic brain changes. *Nat. Commun.* **11**, 812 (2020).
5. Khalil, M. et al. Neurofilaments as biomarkers in neurological disorders - towards clinical application. *Nat. Rev. Neurol.* **20**, 269–287 (2024).
6. Alagaratnam, J. et al. Correlation between cerebrospinal fluid and plasma neurofilament light protein in treated HIV infection: results from the COBRA study. *J. Neurovirol* **28**, 54–63 (2022).
7. Khalil, M. et al. Neurofilaments as biomarkers in neurological disorders. *Nat. Rev. Neurol.* **14**, 577–589 (2018).
8. Bacioglu, M. et al. Neurofilament light chain in blood and CSF as marker of disease progression in mouse models and in neurodegenerative diseases. *Neuron* **91**, 56–66 (2016).
9. Niu, L. D. et al. Genome-wide association study of cerebrospinal fluid neurofilament light levels in non-demented elders. *Ann. Transl. Med*. **7**, 657 (2019).
10. Li, J. Q. et al. Genome-wide association study identifies two loci influencing plasma neurofilament light levels. *BMC Med. Genomics* **11**, 47 (2018).
11. Hong, S. et al. TMEM106B and CPOX are genetic determinants of cerebrospinal fluid Alzheimer's disease biomarker levels. *Alzheimers Dement* **17**, 1628–1640 (2021).
12. Wuttke, M. et al. A catalog of genetic loci associated with kidney function from analyses of a million individuals. *Nat. Genet.* **51**, 957–972 (2019).
13. Yang, J. et al. Conditional and joint multiple-SNP analysis of GWAS summary statistics identifies additional variants influencing complex traits. *Nat. Genet.* **44**, 369–375 (2012).
14. Kunkle, B. W. et al. Genetic meta-analysis of diagnosed Alzheimer's disease identifies new risk loci and implicates Aβ, tau, immunity and lipid processing. *Nat. Genet.* **51**, 414–430 (2019).
15. Nalls, M. A. et al. Identification of novel risk loci, causal insights, and heritable risk for Parkinson's disease: a meta-analysis of genome-wide association studies. *Lancet Neurol.* **18**, 1091–1102 (2019).
16. Yu, Y. et al. Characterization of the GufA subfamily member SLC39A11/Zip11 as a zinc transporter. *J. Nutr. Biochem* **24**, 1697–1708 (2013).
17. Landers, J. E. et al. Reduced expression of the Kinesin-Associated Protein 3 (KIFAP3) gene increases survival in sporadic amyotrophic lateral sclerosis. *Proc. Natl Acad. Sci. USA* **106**, 9004–9009 (2009).
18. Xie, T. et al. Genome-wide association study combining pathway analysis for typical sporadic amyotrophic lateral sclerosis in Chinese Han populations. *Neurobiol. Aging* **35**, 1778.e1779–1778.e1723 (2014).
19. Kanehisa, M. & Goto, S. KEGG: kyoto encyclopedia of genes and genomes. *Nucleic Acids Res*. **28**, 27–30 (2000).
20. Uhlen, M. et al. Proteomics. Tissue-based map of the human proteome. *Science* **347**, 1260419 (2015).
21. Ádori, C. et al. Critical role of somatostatin receptor 2 in the vulnerability of the central noradrenergic system: New aspects on Alzheimer's disease. *Acta Neuropathol.* **129**, 541–563 (2015).
22. Stumm, R. K. et al. Somatostatin receptor 2 is activated in cortical neurons and contributes to neurodegeneration after focal ischemia. *J. Neurosci.* **24**, 11404–11415 (2004).
23. Liu, D. et al. Involvement of mitochondrial K+ release and cellular efflux in ischemic and apoptotic neuronal death. *J. Neurochem* **86**, 966–979 (2003).
24. Korley, F. K. et al. Serum NfL (neurofilament light chain) levels and incident stroke in adults with diabetes mellitus. *Stroke* **50**, 1669–1675 (2019).
25. Akamine, S. et al. Renal function is associated with blood neurofilament light chain level in older adults. *Sci. Rep.* **10**, 20350 (2020).
26. Barro, C., Chitnis, T. & Weiner, H. L. Blood neurofilament light: a critical review of its application to neurologic disease. *Ann. Clin. Transl. Neurol.* **7**, 2508–2523 (2020).
27. Garzone, D. et al. Neurofilament light chain and retinal layers' determinants and association: A population-based study. *Ann. Clin. Transl. Neurol.* **9**, 564–569 (2022).
28. van der Plas, E. et al. Associations between neurofilament light-chain protein, brain structure, and chronic kidney disease. *Pediatr. Res* **91**, 1735–1740 (2022).
29. Scheppach, J. B. et al. Albuminuria and estimated GFR as risk factors for dementia in midlife and older age: Findings from the ARIC study. *Am. J. Kidney Dis.* **76**, 775–783 (2020).
30. Scheppach, J. B. et al. Association of kidney function measures with signs of neurodegeneration and small vessel disease on brain magnetic resonance imaging: The atherosclerosis risk in communities (ARIC) study. *Am. J. Kidney Dis.* **81**, 261–269.e261 (2023).
31. Adam, J. et al. Endoplasmic reticulum stress in UMOD-related kidney disease: A human pathologic study. *Am. J. Kidney Dis.* **59**, 117–121 (2012).
32. Williams, S. E. et al. Uromodulin mutations causing familial juvenile hyperuricaemic nephropathy lead to protein maturation defects and retention in the endoplasmic reticulum. *Hum. Mol. Genet* **18**, 2963–2974 (2009).
33. Zhang, K. & Kaufman, R. J. From endoplasmic-reticulum stress to the inflammatory response. *Nature* **454**, 455–462 (2008).
34. Piperi, C., Adamopoulos, C., Dalagiorgou, G., Diamanti-Kandarakis, E. & Papavassiliou, A. G. Crosstalk between advanced glycation and endoplasmic reticulum stress: emerging therapeutic targeting for metabolic diseases. *J. Clin. Endocrinol. Metab.* **97**, 2231–2242 (2012).
35. Li, H. et al. Crystal and solution structures of human protein-disulfide isomerase-like protein of the testis (PDILT) provide insight into its chaperone activity. *J. Biol. Chem.* **293**, 1192–1202 (2018).
36. Preische, O. et al. Serum neurofilament dynamics predicts neurodegeneration and clinical progression in presymptomatic Alzheimer's disease. *Nat. Med.* **25**, 277–283 (2019).

37. Gudjonsson, A. et al. A genome-wide association study of serum proteins reveals shared loci with common diseases. *Nat. Commun.* **13**, 480 (2022).

38. Manini, A. et al. TMEM106B acts as a modifier of cognitive and motor functions in amyotrophic lateral sclerosis. *Int. J. Mol. Sci.* **23**, https://doi.org/10.3390/ijms23169276 (2022).

39. Bellenguez, C. et al. New insights into the genetic etiology of Alzheimer's disease and related dementias. *Nat. Genet.* **54**, 412–436 (2022).

40. Hu, Y. et al. rs1990622 variant associates with Alzheimer's disease and regulates TMEM106B expression in human brain tissues. *BMC Med.* **19**, 11 (2021).

41. Brady, O. A., Zheng, Y., Murphy, K., Huang, M. & Hu, F. The frontotemporal lobar degeneration risk factor, TMEM106B, regulates lysosomal morphology and function. *Hum. Mol. Genet* **22**, 685–695 (2013).

42. Van Es, M. A. et al. Analysis of FGGY as a risk factor for sporadic amyotrophic lateral sclerosis. *Amyotroph. Lateral Scler.* **10**, 441–447 (2009).

43. Aberg, K. et al. Genomewide association study of movement-related adverse antipsychotic effects. *Biol. Psychiatry* **67**, 279–282 (2010).

44. Daoud, H., Valdmanis, P. N., Dion, P. A. & Rouleau, G. A. Analysis of DPP6 and FGGY as candidate genes for amyotrophic lateral sclerosis. *Amyotroph. Lateral Scler.* **11**, 389–391 (2010).

45. Zhang, Y., Zagnitko, O., Rodionova, I., Osterman, A. & Godzik, A. The FGGY carbohydrate kinase family: Insights into the evolution of functional specificities. *PLoS Comput Biol.* **7**, e1002318 (2011).

46. Dunckley, T. et al. Whole-genome analysis of sporadic amyotrophic lateral sclerosis. *N. Engl. J. Med.* **357**, 775–788 (2007).

47. Mullard, A. NfL makes regulatory debut as neurodegenerative disease biomarker. *Nat. Rev. Drug Discov.* **22**, 431–434 (2023).

48. Garcia, M. L. et al. NF-M is an essential target for the myelin-directed "outside-in" signaling cascade that mediates radial axonal growth. *J. cell Biol.* **163**, 1011–1020 (2003).

49. Campos-Melo, D., Hawley, Z. C. E. & Strong, M. J. Dysregulation of human NEFM and NEFH mRNA stability by ALS-linked miRNAs. *Mol. Brain* **11**, 43 (2018).

50. Lavedan, C., Buchholtz, S., Nussbaum, R. L., Albin, R. L. & Polymeropoulos, M. H. A mutation in the human neurofilament M gene in Parkinson's disease that suggests a role for the cytoskeleton in neuronal degeneration. *Neurosci. Lett.* **322**, 57–61 (2002).

51. Peleg, S. et al. Altered histone acetylation is associated with age-dependent memory impairment in mice. *Science* **328**, 753–756 (2010).

52. Sherva, R. et al. Genome-wide association study of the rate of cognitive decline in Alzheimer's disease. *Alzheimers Dement* **10**, 45–52 (2014).

53. Cronin, S. et al. A genome-wide association study of sporadic ALS in a homogenous Irish population. *Hum. Mol. Genet* **17**, 768–774 (2008).

54. Agís-Balboa, R. C. et al. Formin 2 links neuropsychiatric phenotypes at young age to an increased risk for dementia. *Embo j.* **36**, 2815–2828 (2017).

55. Sun, L. et al. Genome-wide DNA methylation profiles of autism spectrum disorder. *Psychiatr. Genet* **32**, 131–145 (2022).

56. Wexler, E. M. et al. Genome-wide analysis of a Wnt1-regulated transcriptional network implicates neurodegenerative pathways. *Sci. Signal* **4**, ra65 (2011).

57. Qian, L. et al. β2-adrenergic receptor activation prevents rodent dopaminergic neurotoxicity by inhibiting microglia via a novel signaling pathway. *J. Immunol.* **186**, 4443–4454 (2011).

58. Peterson, L., Ismond, K. P., Chapman, E. & Flood, P. Potential benefits of therapeutic use of β2-adrenergic receptor agonists in neuroprotection and Parkinsonụs disease. *J. Immunol. Res.* **2014**, 103780 (2014).

59. Oksanen, M. et al. Astrocyte alterations in neurodegenerative pathologies and their modeling in human induced pluripotent stem cell platforms. *Cell Mol. Life Sci.* **76**, 2739–2760 (2019).

60. Park, H. M. et al. The CRL3(gigaxonin) ubiquitin ligase-USP15 pathway governs the destruction of neurofilament proteins. *Proc. Natl Acad. Sci. USA* **120**, e2306395120 (2023).

61. Dubiel, W., Dubiel, D., Wolf, D. A. & Naumann, M. Cullin 3-based ubiquitin ligases as master regulators of Mammalian cell differentiation. *Trends Biochem Sci.* **43**, 95–107 (2018).

62. Auton, A. et al. A global reference for human genetic variation. *Nature* **526**, 68–74 (2015).

63. McCarthy, S. et al. A reference panel of 64,976 haplotypes for genotype imputation. *Nat. Genet.* **48**, 1279–1283 (2016).

64. Winkler, T. W. et al. Quality control and conduct of genome-wide association meta-analyses. *Nat. Protoc.* **9**, 1192–1212 (2014).

65. Willer, C. J., Li, Y. & Abecasis, G. R. METAL: fast and efficient meta-analysis of genomewide association scans. *Bioinformatics* **26**, 2190–2191 (2010).

66. Mägi, R. et al. Trans-ethnic meta-regression of genome-wide association studies accounting for ancestry increases power for discovery and improves fine-mapping resolution. *Hum. Mol. Genet* **26**, 3639–3650 (2017).

67. Watanabe, K., Taskesen, E., van Bochoven, A. & Posthuma, D. Functional mapping and annotation of genetic associations with FUMA. *Nat. Commun.* **8**, 1826 (2017).

68. Watanabe, K., Umićević Mirkov, M., de Leeuw, C. A., van den Heuvel, M. P. & Posthuma, D. Genetic mapping of cell type specificity for complex traits. *Nat. Commun.* **10**, 3222 (2019).

69. Pruim, R. J. et al. LocusZoom: regional visualization of genome-wide association scan results. *Bioinformatics* **26**, 2336–2337 (2010).

70. Bulik-Sullivan, B. K. et al. LD Score regression distinguishes confounding from polygenicity in genome-wide association studies. *Nat. Genet* **47**, 291–295 (2015).

71. de Leeuw, C. A., Mooij, J. M., Heskes, T. & Posthuma, D. MAGMA: generalized gene-set analysis of GWAS data. *PLoS Comput Biol.* **11**, e1004219 (2015).

72. Lonsdale, J. et al. The Genotype-Tissue Expression (GTEx) project. *Nat. Genet.* **45**, 580–585 (2013).

73. CAG repeat not polyglutamine length determines timing of Huntington's disease onset. *Cell* **178**, 887–900.e814 (2019).

74. van Rheenen, W. et al. Common and rare variant association analyses in amyotrophic lateral sclerosis identify 15 risk loci with distinct genetic architectures and neuron-specific biology. *Nat. Genet* **53**, 1636–1648 (2021).

75. Damotte, V. et al. Plasma amyloid β levels are driven by genetic variants near APOE, BACE1, APP, PSEN2: A genome-wide association study in over 12,000 non-demented participants. *Alzheimers Dement* **17**, 1663–1674 (2021).

76. Sarnowski, C. et al. Meta-analysis of genome-wide association studies identifies ancestry-specific associations underlying circulating total tau levels. *Commun. Biol.* **5**, 336 (2022).

77. van der Meer, D. et al. Brain scans from 21,297 individuals reveal the genetic architecture of hippocampal subfield volumes. *Mol. Psychiatry* **25**, 3053–3065 (2020).

78. Zhao, B. et al. Genome-wide association analysis of 19,629 individuals identifies variants influencing regional brain volumes and refines their genetic co-architecture with cognitive and mental health traits. *Nat. Genet* **51**, 1637–1644 (2019).

79. Sargurupremraj, M. et al. Cerebral small vessel disease genomics and its implications across the lifespan. *Nat. Commun.* **11**, 6285 (2020).

80. MacArthur, J. et al. The new NHGRI-EBI Catalog of published genome-wide association studies (GWAS Catalog). *Nucleic Acids Res.* **45**, D896–d901 (2017).

81. Choi, S. W. & O'Reilly, P. F. PRSice-2: Polygenic risk score software for biobank-scale data. *Gigascience* **8**, https://doi.org/10.1093/gigascience/giz082 (2019).

82. Giambartolomei, C. et al. Bayesian test for colocalisation between pairs of genetic association studies using summary statistics. *PLoS Genet* **10**, e1004383 (2014).

83. Liu, B., Gloudemans, M. J., Rao, A. S., Ingelsson, E. & Montgomery, S. B. Abundant associations with gene expression complicate GWAS follow-up. *Nat. Genet.* **51**, 768–769 (2019).

84. Hemani, G. et al. The MR-Base platform supports systematic causal inference across the human phenome. *Elife* **7**, https://doi.org/10.7554/eLife.34408 (2018).

85. Bowden, J., Davey Smith, G., Haycock, P. C. & Burgess, S. Consistent estimation in Mendelian randomization with some invalid instruments using a weighted median estimator. *Genet Epidemiol.* **40**, 304–314 (2016).

86. Bowden, J., Davey Smith, G. & Burgess, S. Mendelian randomization with invalid instruments: Effect estimation and bias detection through Egger regression. *Int J. Epidemiol.* **44**, 512–525 (2015).

87. Bowden, J. et al. Improving the visualization, interpretation and analysis of two-sample summary data Mendelian randomization via the Radial plot and Radial regression. *Int. J. Epidemiol.* **47**, 1264–1278 (2018).

Author contributions

S.A., S.S., N.A.A., M.G. and M.Ar.I. Study design and drafting of the manuscript. S.A and M.A.I. writing and editing. S.A., M.A.I., A.M., R.W., M.H.R., J.C.B., M.F., G.R., E.H., M.W.L., WT.L.Jr., R.X., V.B., T.H.M., L.L., M.K., J.K., R.A.R., G.C., C.D., L.D., M.J.L., K.M., W.S.K., C.E.F., R.S., S.D., M.M.B., K.B., Q.Y., S.S., N.A.A., M.G. and M.Ar.I. Statistical analysis, interpretation of data and revision of the manuscript. J.C.B., M.F., T.H.M., L.L., C.D., L.D., M.J.L., K.M., W.S.K., C.E.F., R.S., S.D., M.M.B., K.B., Q.Y., S.S., N.A.A., M.G. and M.Ar.I. Acquisition of the data.

Competing interests

The authors declare no competing interests.

Additional information

Publisher's note Springer Nature remains neutral with regard to jurisdictional claims in published maps and institutional affiliations.

[1]Department of Epidemiology, Erasmus University Medical Center, PO Box 2040, 3000 CA Rotterdam, the Netherlands. [2]Oxford-GSK Institute of Computational and Molecular Medicine (IMCM), Centre for Human Genetics, Nuffield Department of Medicine (NDM), University of Oxford, Oxford OX3 7BN, UK. [3]Population Health Sciences, German Center for Neurodegenerative Diseases (DZNE), Venusberg-Campus 1/99, 53127 Bonn, Germany. [4]University of Bordeaux, Inserm, Bordeaux Population Health Research Center, UMR 1219, F-33000 Bordeaux, France. [5]Boston University, Boston, MA 02215, USA. [6]Department of Genetic Epidemiology, Institute of Human Genetics, University of Münster, Münster, Germany. [7]Department of Psychiatry, University of Münster, Münster, Germany. [8]Cardiovascular Health Research Unit, Department of Medicine, University of Washington, 1730 Minor Ave #1360, Seattle, WA 98101, USA. [9]Brown Foundation Institute of Molecular Medicine, McGovern Medical School, University of Texas Health Science Center at Houston, 1825 Pressler Street Houston, Houston 77030 TX, USA. [10]Clinical Division of Neurogeriatrics, Department of Neurology, Medical University of Graz, Auenbruggerplatz 22, 8036 Graz, Austria. [11]Institute for Medical Informatics, Statistics and Documentation, Medical University of Graz, Auenbruggerplatz 2, Fifth Floor, Graz 8036, Austria. [12]National Center for PTSD, Behavioral Sciences Division at VA Boston Healthcare System, Boston, 150 South Huntington Avenue, Boston, MA 02130, USA. [13]Department of Psychiatry and Biomedical Genetics, Boston University School of Medicine, Boston, 72 East Concord Street E200, Boston, MA 02118, USA. [14]Departments of Neurology and Epidemiology, University of Washington, Seattle, 3980 15th Ave NE Seattle, Seattle, WA 98195, USA. [15]MIND Center, University of Mississippi Medical Center, Jackson, 2500 North State Street, Jackson, MS 39216, USA. [16]Laboratory of Epidemiology and Population Science, NIA Intramural Research Program, 251 Bayview Blvd, Baltimore, MD 21224, USA. [17]Department of Neurology, Medical University of Graz, Auenbruggerplatz 22, 8036 Graz, Austria. [18]Research Center for Clinical Neuroimmunology and Neuroscience University Hospital, Spi-talstrasse 2, CH-4031 Basel, Switzerland. [19]Department of Physiology and Neuroscience, Alzheimer's Therapeutic Research Institute, Keck School of Medicine of the University of Southern California, California, USA. [20]Brigham and Women's Hospital, Harvard Medical School, Boston, 75 FRANCIS STREET, BOSTON MA 02115, MA Boston, USA. [21]Department of Psychological & Brain Sciences, Boston University, Boston, 64 Cummington Mall # 149, Boston, MA 02215, USA. [22]Beth Israel Deaconess Medical Center, Harvard Medical School, Boston330 Brookline Avenue BostonMA 02215, USA. [23]Department of Psychiatry and Center for Behavior Genetics of Aging, University of California, San Diego, La Jolla, CA 92093, USA. [24]CHU de Bordeaux, Department of Neurology, Institute for Neurodegenerative Diseases, F-33000 Bordeaux, France. [25]Institute for Medical Biometry, Informatics and Epidemiology (IMBIE), Faculty of Medicine, University of Bonn, Venusberg-Campus 1, 53127 Bonn, Germany. [26]Institute of Epidemiology and Social Medicine, University of Münster, Münster, Institut für Epidemiologie und Sozialmedizin Albert-Schweitzer-Campus 1, Gebäude D3 48149, Münster, Germany. [27]Glenn Biggs Institute for Alzheimer's and Neurodegenerative Diseases, University of Texas Health Sciences Center, San Antonio, TX, USA. [28]Department of Neurology, Faculty of Medicine, University of Bonn, 53127 Bonn, Germany. [29]These authors contributed equally: Shahzad Ahmad, Mohammad Aslam Imtiaz. [30]These authors jointly supervised this work: N. Ahmad Aziz, Mohsen Ghanbari, M. Arfan Ikram. ✉e-mail: m.a.ikram@erasmusmc.nl